quadruply bonded metal dimer, (ii) predict an Re-Re quadruple bond energy of 85 ± 5 kcal/mol—the first direct estimate of the strength of this prototypical quadruple bond, and (iii) suggest that the δ bond energy is 6 ± 3 kcal/mol.

Acknowledgment. We acknowledge Dr. Siddharth Dasgupta for his contributions in the vibrational analysis. This work was partially supported by grants from the Sun Co. and from National Science Foundation (No. CHE83-18041).

Ligand-Aided Photoreduction of Iron-Porphyrin Complexes Probed by Resonance Raman Spectroscopy

Y. Ozaki,[1a] K. Iriyama,[1a] H. Ogoshi,[1b] and T. Kitagawa*[1c]

Contribution from the Division of Biochemistry, The Jikei University School of Medicine, Nishi-shinbashi, Minato-ku, Tokyo, 105 Japan, Department of Chemistry and Chemical Engineering, The Technological University of Nagaoka, Nagaoka, 949-54 Japan, and Institute for Molecular Science, Okazaki National Research Institutes, Myodaiji, Okazaki, 444 Japan.
Received June 30, 1986

Abstract: Photoreduction has been observed for the first time for an iron porphyrin with a biologically relevant axial ligand by using resonance Raman (RR) spectroscopy (for Fe^{III}(OEP)(2-MeIm), OEP = octaethylporphyrin and 2-MeIm = 2-methylimidazole). The action spectrum for the photoreduction obtained by visible absorption spectra exhibited a broad maximum around 420–460 nm, which was appreciably shifted from the Soret band of Fe^{III}(OEP)(2-MeIm) at 395 nm. Similar photoreduction was observed for Fe^{III}(OEP)(1,2-Me_2Im) (1,2-Me_2Im = 1,2-dimethylimidazole) but not for Fe^{III}(OEP)L_2 (L = imidazole and 1-methylimidazole) and Fe^{III}(OEP)X (X = F, Cl, Br, I, and ClO_4). The coincidence of the RR spectrum of the photoreduced species with that of the ferrous porphyrin rules out the possibility of ring reduction to a porphyrin anion radical or chlorin. The dependence of the photoreduction on the concentration of 2-MeIm suggested that the ligand-free Fe^{II}(OEP) is a likely intermediate and thus that the light-induced charge transfer from the axial ligand to the iron ion is the primary process of photoreduction.

In the resonance Raman (RR) studies of some hemeproteins, occurrence of photoreduction has been noticed upon laser irradiation at selected wavelengths,[2-8] but nothing is known about its mechanism and electron donors. Apart from those studies, the photoreduction has been explored for several metalloporphyrins from the view of photochemistry,[9-15] although no Raman study has been included. To gain an insight into the photoreduction mechanism of hemeproteins, we investigated iron porphyrin complexes with a biologically relevant axial ligand by using RR spectroscopy. The use of this technique might allow us to infer an intermediate molecular species involved in the photoreduction on the basis of the accumulated knowledge about the RR spectra of iron porphyrins.[16,17] Here we report RR evidence for photoreduction of 2-methylimidazole (2-MeIm) and 1,2-dimethylimidazole (1,2-Me_2Im) complexes of iron-octaethylporphyrin [Fe^{III}(OEP)] and point out the formation of the four-coordinate ferrous complex as an intermediate.

Experimental Procedures

Fe^{III}(OEP)X (X = F, Cl, Br, I, and ClO_4) were synthesized with the methods described elsewhere.[18,19] 2-MeIm was recrystallized just before use, and its ^{1}H NMR spectrum showed that it did not contain any detectable impurity. The procedures for preparing the alkyl-imidazole complexes of Fe^{III}(OEP)X and Fe^{II}(OEP)(2-MeIm) were described previously.[20] As a solvent dichloromethane (CH_2Cl_2) of spectroscopic grade (Wako, Osaka) was used without further purification. All solutions were degassed unless otherwise stated and kept at 10 °C during the Raman measurements.

Raman spectra were measured with a JEOL-400D Raman spectrometer equipped with an RCA-31034a photomultiplier. The excitation sources used are Kr^+ (Spectra Physics, Model 164), He/Cd (Kinmon Electrics, Model CDR80MGE), and Ar^+ (NEC, Model GLG3200) lasers. Raman shifts were calibrated with indene, and errors of peak frequencies would be less than 1 cm^{-1} for well defined bands. Conventional absorption spectra were recorded with a Hitachi 124S spectrophotometer.

To determine an action spectrum of photoreduction, the degassed solution of Fe^{III}(OEP)(2-MeIm) was placed in a water bath at 20 °C and illuminated by a projector lamp for 5 min in the presence of short cut filters including Y-48, Y-46, Y-44, L-42, L-40, and L-38 (Hoya Corp.). For every measurement a fresh sample from the same stock solution was prepared and their absorption spectra were observed. Since the short cut filter specified by λ_1 allows light with the wavelength longer than λ_1 to pass, the difference between the spectra observed in the presence of the filters, λ_1 and λ_2, which is designated by $S(\lambda_1 - \lambda_2)$, represents the effect of the illumination of light with the wavelengths between λ_1 and λ_2. For

* Author to whom correspondences should be addressed.

(1) (a) The Jikei University School of Medicine. (b) Technological University of Nagaoka. (c) Institute for Molecular Science.
(2) Kitagawa, T.; Orii, Y., *J. Biochem. (Tokyo)* **1978**, *84*, 1245.
(3) Adar, F.; Yonetani, T. *Biochim. Biophys. Acta*, **1978**, *502*, 80.
(4) Salmeen, I.; Rimai, L.; Babcock, G. T. *Biochemistry* **1978**, *17*, 800.
(5) Ogura, T.; Sone, N.; Tagawa, K.; Kitagawa, T. *Biochemistry*, **1984**, *23*, 2826.
(6) Kitagawa, T.; Nagai, K. *Nature (London)* **1979**, *281*, 503.
(7) Kitagawa, T.; Chihara, S.; Fushitani, K.; Morimoto, H. *J. Am. Chem. Soc.* **1984**, *106*, 1860.
(8) Yoshikawa, S.; Mochizuki, H.; Chihara, S.; Hagihara, B.; Kitagawa, T. *Biochim. Biophys. Acta*, **1984**, *786*, 267.
(9) Harriman, A.; Porter, G. *J. Chem. Soc., Faraday Trans.* **1979**, *75*, 1543.
(10) Bartocci, C.; Scandola, F.; Ferri, A.; Carassiti, V., *J. Am. Chem. Soc.* **1980**, *102*, 7067.
(11) Bizet, C.; Morliere, P.; Brault, D.; Delgado, O.; Bazin, M.; Santus, R. *Photochem. Photobiol.* **1981**, *34*, 315.
(12) Bartocci, C.; Maldotti, A.; Traverso, O.; Bignozzi, C. A.; Carassiti, V. *Polyhedron* **1983**, *2*, 97.
(13) Maldotti, A.; Bartocci, C.; Amadelli, R.; Carassiti, V. *Inorg. Chem. Acta* **1983**, *74*, 275.
(14) Hoshino, M.; Konishi, S.; Imamura, M. *Bull. Chem. Soc. Jpn.* **1984**, *57*, 1713.
(15) Imamura, T.; Jin, T.; Suzuki, T.; Fujimoto, M. *Chem. Lett.* **1985**, 847.
(16) Kitagawa, T.; Ozaki, Y. In *Structure and Bonding* **1987**, *64*, 71.
(17) Spiro, T. G. In *Iron Porphyrins*; Lever, A. B. P., Gray, H. B., Eds.; Addison-Wesley: Reading, 1983; Vol. 2, p 91.
(18) Ogoshi, H.; Watanabe, E.; Yoshida, Z.; Kincaid, J.; Nakamoto, K. *J. Am. Chem. Soc.* **1973**, *95*, 2845.
(19) Ogoshi, H.; Sugimoto, H.; Yoshida, Z. *Bull. Chem. Soc. Jpn.* **1981**, *54*, 3414.
(20) Ozaki, Y.; Iriyama, K.; Ogoshi, H.; Ochiai, T.; Kitagawa, T. *J. Phys. Chem.* **1986**, *90*, 6105.

0002-7863/87/1509-5583$01.50/0

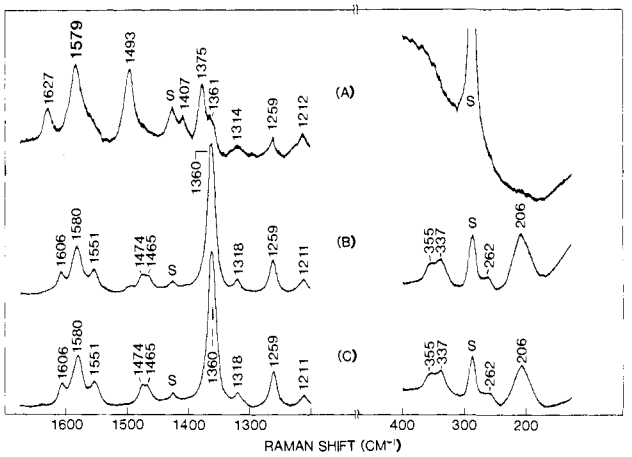

Figure 1. The 441.6-nm excited RR spectrum of Fe^{III}(OEP)(2-MeIm) in CH_2Cl_2 and its photoreduced and chemically reduced species. (A) Fe^{III}(OEP)(2-MeIm) under aerobic conditions; sensitivity, 250 counts/s; scan speed, 10 cm^{-1}/min; time constant, 8 s; laser, 30 mW. (B) The same sample as in part A but under anaerobic conditions; sensitivity, 2500 counts/s; scan speed, 50 cm^{-1}/min; time constant, 2 s; laser, 45 mW. (C) Dithionite-reduced species under anaerobic conditions. Instrumental conditions are the same as those in part B. Fe^{III}(OEP)(2-MeIm) was provided by mixing Fe^{III}(OEP)I (1.85 mM) with 2-MeIm (185 mM) (the final concentrations) for all samples.

measuring the relative intensity of the illuminating light, the filter-transmitted projector light was dispersed with a 10-cm monochromator (Ritsu Ohyo Kokagu, MN-10C), which has a 500-nm blaze and 1200-gr/mm grating, and detected with a pin photodiode (Hamamatsu, S1722-02).[21] After observation of the transmission spectra of individual filters, difference spectra, $D(\lambda_1 - \lambda_2)$, between two spectra obtained in the presence of the filters, λ_1 and λ_2, were calculated and corrected on the basis of the inherent wavelength dependences of the monochromator transmittance and of the detector sensitivity. To convert the light energy into the relative number of photons, the integral of $\lambda D(\lambda_1 - \lambda_2)$ was calculated with the partial integration method by dividing the region between λ_1 and λ_2 into ten segments.

Results and Discussion

Figure 1A shows the 441.6-nm excited RR spectrum of Fe^{III}(OEP)(2-MeIm) in CH_2Cl_2 measured under aerobic conditions. The ν_4, ν_3, and ν_{10} bands at 1375, 1493, and 1627 cm^{-1}, respectively, indicate the complex is a five-coordinate ferric high-spin species. The frequencies of Raman bands around 1500–1650 cm^{-1} can be used to distinguish between Fe^{III}(OEP)L (L = 2-MeIm or 1,2-Me_2Im) and Fe^{III}(OEP)X (X = F, Cl, or Br).[20] When the sample which gave the spectrum of Figure 1A was placed under anaerobic conditions ($\sim 10^{-2}$ mmHg), the ν_4, ν_3, and ν_{10} bands were shifted to 1360, 1474, and 1606 cm^{-1}, respectively, as shown by trace B, and its overall spectral pattern as well as the frequencies of the marker bands is almost identical with those of the chemically prepared Fe^{II}(OEP)(2-MeIm), the spectrum of which is shown by trace C. This observation clearly demonstrates that Fe^{III}(OEP)(2-MeIm) is photoreduced to Fe^{II}(OEP)(2-MeIm) upon irradiation of laser light at 441.6 nm. This occurred with a laser powder as low as 10 mW. The photoreduction takes place even under aerobic conditions, but since the photoreduced species are reoxidized immediately, the aerobic laser irradiation brings about a photo-steady state. The shoulder at 1361 cm^{-1} in Figure 1A is due to the photoreduced species present in the photosteady state. Note that the Fe^{II}–(2-MeIm) stretching mode is seen at 206 cm^{-1} for the photoreduced species as for the chemically reduced species.

Similar experiments were carried out with various laser lines; the irradiation at 406.7 nm provided the same result as that at 441.6 nm, but the irradiation at 488.0 and 514.5 nm gave rise to a mixture of the photoreduced and unreduced species. Therefore, the photoreduction depends on the irradiation wavelength as was so for hemeproteins.[2-8] The photoreduction was

(21) Ogura, T.; Kitagawa, T., to be published.

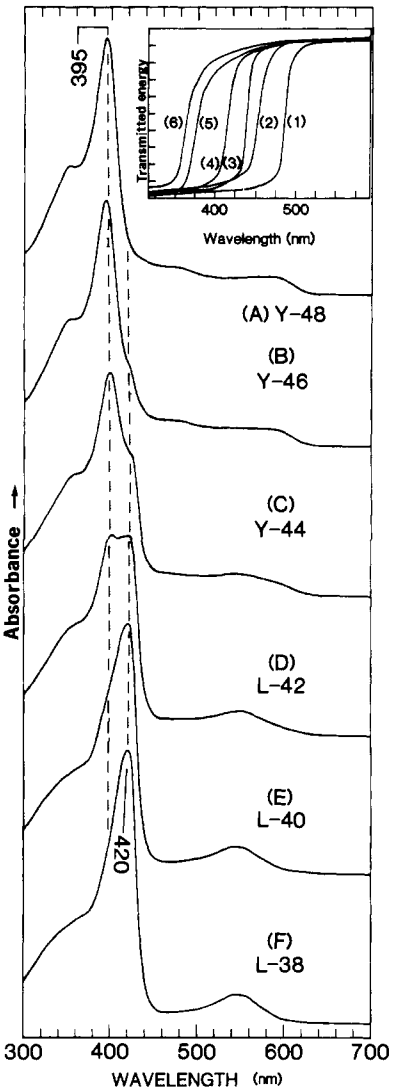

Figure 2. Visible absorption spectra of Fe^{III}(OEP)(2-MeIm) in CH_2Cl_2 illuminated by a projector lamp for 5 min through the designated short cut filters. The inset figure illustrates the spectra of the illuminated light specified by the short cut filters; (1), (2), (3), (4), (5), and (6) correspond to Y-48, Y-46, Y-44, L-42, L-40, and L-38, respectively. The intensity is not normalized and, therefore, the spectral intensity also reflects the spectrum of the projector lamp.

apparently retarded when the spinning cell (1800 rpm) was used under an Ar atmosphere, but it definitely took place. Since the resonance enhancement of Raman intensity is different between the ferric and ferrous complexes, the relative intensity of Raman bands of the photoreduced and unreduced species cannot serve as a quantitative measure of occurrence of photoreduction.

The photoreduction was ascertained by the UV–visible absorption spectra; when a degassed CH_2Cl_2 solution of Fe^{III}(OEP)(2-MeIm) was illuminated by a projector lamp for 10 min without any filters, the spectrum was identical with that of Fe^{II}(OEP)(2-MeIm). To clarify the dependence of the photoreduction on the wavelength of the illuminated light, the experiments for determining the action spectrum were carried out. Figure 2 shows the absorption spectra of the samples illuminated in the presence of the denoted filters. Absorptions at 395 and 420 nm arise from Fe^{III}(OEP)(2-MeIm) and its photoreduced product, respectively. The inset figure illustrates the spectra of the illuminated light for photoreduction, which are represented with an identical scale.

The difference spectra, $S(\lambda_1 - \lambda_2)$, were calculated as shown in Figure 3A. The difference spectra of the illuminated light, $D(\lambda_1 - \lambda_2)$, are depicted at the right side of each difference absorption spectrum in Figure 3B, where scales of the ordinates are common to all spectra within $S(\lambda_1 - \lambda_2)$ or $D(\lambda_1 - \lambda_2)$. Il-

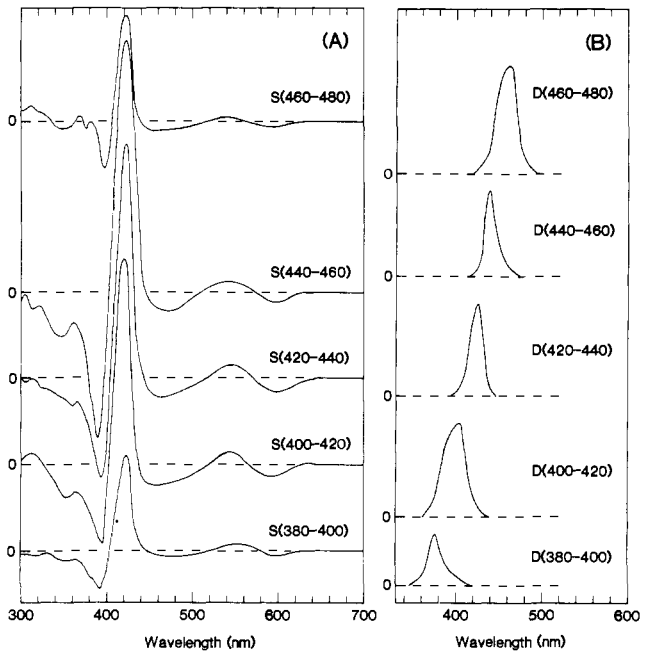

Figure 3. (A) Difference spectra for the absorption spectra shown in Figure 2. (B) Difference, $D(\lambda_1 - \lambda_2)$, for the spectra of the illuminated light shown in the inset of Figure 2. $S(\lambda_1 - \lambda_2)$ and $D(\lambda_1 - \lambda_2)$ represent the difference between the spectra observed in the presence of the short cut filters, λ_1 and λ_2. The ordinate scales are the same within $S(\lambda_1 - \lambda_2)$ or $D(\lambda_1 - \lambda_2)$.

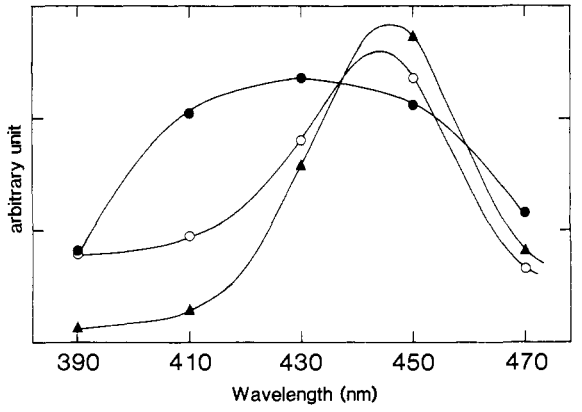

Figure 4. Action spectrum and relative quantum yield for photoreduction of Fe^{III}(OEP)(2-MeIm) in CH_2Cl_2; closed circles show raw data obtained simply by measuring the peak height at 420 nm, ΔI_{420}, in Figure 3; open circles show the relative magnitude of $\Delta I_{420}/[\lambda D(\lambda_1 - \lambda_2)]$ after correction of $D(\lambda_1 - \lambda_2)$ with regard to the wavelength dependence of the transmittance efficiency of the monochromator and of detector sensitivity; closed triangles show the relative quantum yield for the photoreduction. To obtain the yield the values of the open circles were divided by the absorbance of Fe^{III}(OEP)(2-MeIm) at $(\lambda_1 + \lambda_2)/2$. The points for $S(\lambda_1 - \lambda_2)$ and $D(\lambda_1 - \lambda_2)$ are plotted at $(\lambda_1 + \lambda_2)/2$ of the abscissa.

lumination of light corresponding to $D(\lambda_1 - \lambda_2)$ caused the absorption differences, $S(\lambda_1 - \lambda_2)$. It is evident that the absorption intensity at 420 nm becomes largest upon illumination around 420–460 nm.

The peak intensities at 420 nm in $S(\lambda_1 - \lambda_2)$ in Figure 3 are plotted against the illuminated wavelength in Figure 4, where the data for $S(\lambda_1 - \lambda_2)$ are located at $(\lambda_1 + \lambda_2)/2$ of the abscissa. The closed circles stand for the raw data from Figure 3, and the open circles represent the values after the illuminated light energy is corrected and converted into the photon numbers. The action spectrum thus obtained exhibited a broad maximum around 420–460 nm, which is appreciably shifted from the Soret band of Fe^{III}(OEP)(2-MeIm) at 395 nm. This broad maximum might indicate a charge-transfer band from 2-MeIm to Fe^{III}. To deduce a quantum yield for photoreduction, the corrected values of $\lambda D(\lambda_1 - \lambda_2)$ [λ is the wavelength] were divided by the absorbance at $(\lambda_1 + \lambda_2)/2$ of the oxidized form and are plotted in the same figure by triangular markers. The peak position does not shift in this case, although the values became lower at shorter wavelengths due to larger absorbance.

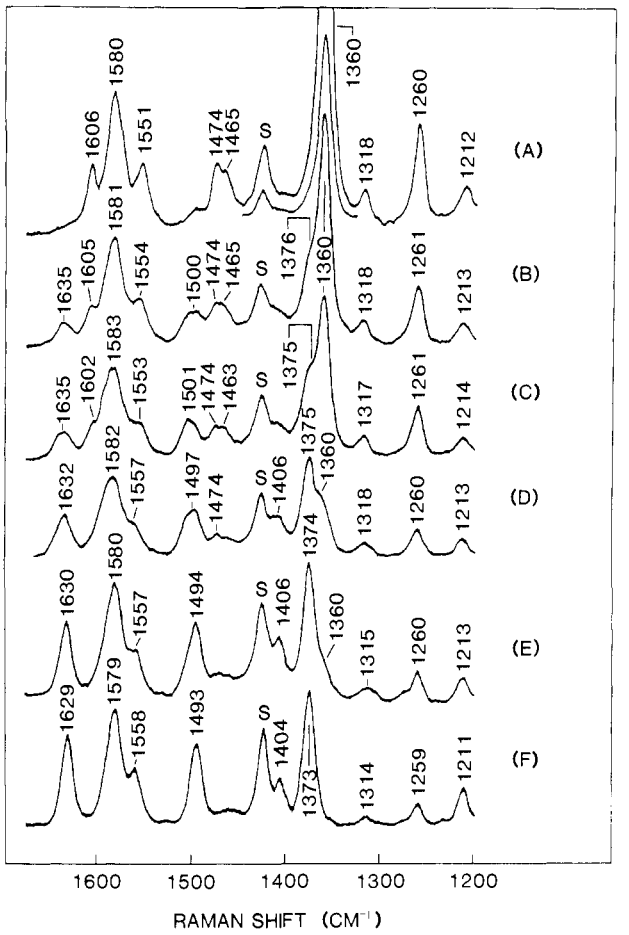

Figure 5. Dependence of the photoreduction on the concentration of 2-MeIm. Raman spectra were observed for the anaerobic mixture of Fe^{III}(OEP)I (1.75 mM) with the CH_2Cl_2 solutions of 2-MeIm having different concentrations by using the 441.6-nm excitation line (30 mW). The concentration of 2-MeIm is as follows: (A) 175, (B) 43.8, (C) 17.5, (D) 4.38, (E) 1.75, (F) 0 mM.

The photoreduction was also observed for Fe^{III}(OEP)(1,2-Me_2Im). However, Fe^{III}(OEP)$(Im)_2$ (Im = imidazole) and Fe^{III}(OEP)$(1\text{-MeIm})_2$ (1-MeIm = 1-methylimidazole) were not photoreduced at all under the same experimental conditions. Phenomenologically, it seems that the five-coordinate high-spin complexes undergo photoreduction but the six-coordinate low-spin complexes do not. It is noteworthy that, even with the five-coordinate complexes, Fe^{III}(OEP)X (X = F, Cl, Br, I, and ClO_4) in the absence of 2-MeIm or 1,2-Me_2Im did not undergo the photoreduction, but in their presence the photoreduction occurred equally irrespective of X = F, Cl, Br, I, or ClO_4. The iron–octaethylchlorin complexes [Fe^{III}(OEC)L] exhibited photoreduction similar to that of the Fe^{III}(OEP)L complexes. The photoreduced product of Fe^{III}(OEP)(2-MeIm) is different from Fe^{III}(OEC)(2-MeIm) and its photoproduct, Fe^{II}(OEC)(2-MeIm), indicating that the porphyrin ring is not reduced.

In order to elucidate the photoreduction mechanism of Fe^{III}-(OEP)(2-MeIm), the dependence of the photoreduction on the concentration of 2-MeIm was investigated. Figure 5 shows the 441.6-nm excited RR spectra of the mixture of Fe^{III}(OEP)I with 2-MeIm; the concentration of 2-MeIm is 175 (5A), 43.8 (5B), 17.5 (5C), 4.38 (5D), 1.75 (5E), and 0 mM (5F), while the concentration of Fe^{III}(OEP)I is kept at 1.75 mM. Spectrum 5A is exactly the same as that of Fe^{II}(OEP)(2-MeIm). Spectrum 5E is very close to that of Fe^{III}(OEP)I (Figure 5F), but there is a shoulder at 1360 cm^{-1} that is assignable to the ν_4 mode of Fe^{II}(OEP)(2-MeIm). In comparison of spectrum 5D with that

of 5E, the intensity of the shoulder at 1360 cm^{-1} increases markedly and the characteristic band of the ferrous high-spin species grows at 1474 cm^{-1}. Of particular interest in spectrum 5D are the upward shifts of the ν_{10}, ν_2, and ν_3 bands; these bands are identified at 1632, 1582, and 1497 cm^{-1}, respectively, for spectrum 5D, and at 1630, 1580, and 1494 cm^{-1} for spectrum 5E. It should be kept in mind that the corresponding bands have been observed at 1629, 1579, and 1493 cm^{-1} for Fe^{III}(OEP)I (Figure 5F), at 1627, 1579, and 1493 cm^{-1} for Fe^{III}(OEP)(2-MeIm) (Figure 1A), and at 1606, 1580, and 1474 cm^{-1} for Fe^{II}-(OEP)(2-MeIm) (Figure 5A). Therefore, the upward-shifted frequencies of the ν_{10}, ν_2, and ν_3 bands cannot be accounted for by a change of the spectral contributions from these three species. The broad feature of these bands in spectrum 5D increased steady-state concentration of an intermediate, which should have the three bands at higher frequencies than those of the three complexes cited above. The three bands are shifted to further higher frequencies in spectrum 5C, suggesting that the relative spectral contribution from the intermediate increases in spectrum 5C. In spectrum 5B, however, the intensities of the ν_{10} and ν_3 bands slightly decrease, and the ν_2 band exhibits a downward shift, probably due to the decreased contribution from the intermediate. Taking account of the presence of band-overlapping, it seems most likely to locate the ν_{10} and ν_3 bands of the intermediate at 1635-1640 and 1500-1505 cm^{-1}, respectively.

The well-known correlation of the RR frequencies of the ν_{10} and ν_3 bands with a structure of iron-porphyrin[16,17] allows us to deduce that the intermediate adopts the ferric low-spin or ferrous intermediate-spin state. Since Fe^{III}(OEP)I does not give a low-spin complex with 2-MeIm under the present condition,[22] it is very unlikely to assign the intermediate to the ferric low-spin species. Consequently, we infer that the intermediate is the intermediate-spin Fe^{II}(OEP) with no axial ligand. In fact, Fe^{II}(OEP) is known to give the ν_{10} and ν_3 bands at 1640 and 1504 cm^{-1}, respectively.[23] Thus the following mechanism appears plausible

$$Fe^{III}(OEP)X \rightarrow Fe^{III}(OEP)(2\text{-MeIm}) \overset{h\nu}{\rightleftharpoons} Fe^{II}(OEP) \rightleftharpoons Fe^{II}(OEP)(2\text{-MeIm})$$

The light excitation of Fe^{III}(OEP)(2-MeIm) causes a charge transfer from 2-MeIm to Fe^{III}(OEP), inducing the dissociation of 2-$MeIm^+$ from the axial coordination position. When there is an excess of 2-MeIm, another 2-MeIm molecule coordinates to the ligand free Fe^{II}(OEP), stabilizing the ferrous high-spin 2-MeIm complex. When the amount of 2-MeIm is too small, Fe^{III}(OEP)(2-MeIm) is not sufficiently supplied. Therefore, the photoreduction depends on the concentration of 2-MeIm. The mechanism described above would be consistent with the observed action spectrum which suggested that the irradiation in the $Fe^{III} \leftarrow$ 2-MeIm CT band was most effective for photoreduction. This sort of mechanism was originally proposed by Bartocci et al.[12] from the ESR spin-trapping experiment for photoreduction of Fe^{III}(PP)(py) (PP = protoporphyrin, py = pyridine). Although their proposal was based on the ESR signals of the leaving ligand, we support this from the Raman signals of porphyrin side. It is unexpected that the Fe^{III}-(2-MeIm) stretching Raman band of Fe^{III}(OEP)(2-MeIm) or internal modes of 2-MeIm were not resonance enhanced upon excitation at 441.6 and 488.0 nm. This may be attributed to very small absorbance of the CT transition.

Acknowledgment. We express our gratitude to Dr. T. Ogura, Institute for Molecular Science, for his help in measuring the action spectrum. This work was supported by the Joint Studies Program (1985) of the Institute for Molecular Science and by a Grant-in-Aid for Scientific Research (61740354) to Y.O. and (60470018) to T.K.

(22) The 441.6-nm excited RR spectrum of the aerobic mixture of Fe^{III}-(OEP)I (1.85 mM) with 2-MeIm (185 mM) shown in Figure 1A demonstrates that Fe^{III}(OEP)I forms exclusively the high-spin complex with 2-MeIm.

(23) Kitagawa, T.; Teraoka, J. *Chem. Phys. Lett.* **1979**, *63*, 443.

Pairwise Additivity in Exciton-Coupled CD Curves of Multichromophoric Systems

William T. Wiesler, Jesús T. Vázquez, and Koji Nakanishi*

Contribution from the Department of Chemistry, Columbia University, New York, New York 10027. *Received December 26, 1986*

Abstract: The general validity of pairwise additivity in exciton split CD curves was demonstrated by using methyl α-D-glucopyranoside as a model system with *p*-bromobenzoate (λ_{max} = 245 nm) and *p*-methoxycinnamate (λ_{max} = 311 nm) esters as chromophores. All 24 possible dichromophore diacetates (six dicinnamates, six dibenzoates, and 12 monocinnamate monobenzoates) were prepared to represent the degenerate and nondegenerate pairwise interactions contributing to the complex CD curves of multichromophoric cases. In the 20 tri- and tetrachromophoric cases prepared to check the additivity, spectral summation of the three or six corresponding constituent pairwise interactions, respectively, yielded excellent empirical calculations of the observed CD curves throughout the 200-400 nm region. The accuracy of such additive calculations provides a general affirmation of the Principle of Pairwise Additivity and justifies a retroadditive approach to spectral interpretation. Application of a "bichromophoric" derivatization to sterochemical problems including glycosidic linkage determinations promises to be a valuable extension of the exciton chirality method.

When a molecule contains two asymmetrically perturbed chromophores, interpretation of ORD and CD spectra have often benefited from an "additive" approach. Djerassi demonstrated that ORD spectra of diketosteroids[1] and diketoterpenes[2] could be calculated empirically by superimposition of the corresponding monoketone dispersion curves, provided that no "vicinal" interaction between the two carbonyl groups occurred. Snatzke later applied this approach to CD spectra of diketo compounds,[3] yet again such an approach was successful only when one keto group

(1) Djerassi, C.; Closson, W. *J. Am. Chem. Soc.* **1956**, *78*, 3761.
(2) Djerassi, C.; Marshall, D.; Nakano, T. *J. Am. Chem. Soc.* **1958**, *80*, 4853.

(3) (a) Snatzke, G.; Fehlhaber, H. W. *Tetrahedron* **1964**, *20*, 1243. (b) Snatzke, G.; Eckhardt, G. *Tetrahedron* **1968**, *24*, 4543.

0002-7863/87/1509-5586$01.50/0